This article has been accepted for publication in IEEE Transactions on Vehicular Technology. This is the author's version which has not been fully edited and content may change prior to final publication. Citation information: DOI 10.1109/TVT.2024.3353348



# Optimal Allocation of Layover Time in a Smart DC Railway Metro Traction System

Marilisa Botte, Luca D'Acierno, Antonio Di Pasquale, Fabio Mottola, *Senior Member, IEEE,* and Mario Pagano, *Senior Member, IEEE*

***Abstract*—In the 2000s, the liberalization of the rail markets for freight and passenger travel opened up the competition. Nowadays, local, regional, and long-distance passenger rail are gradually following suit. As a consequence of the paradigm of realizing smart and sustainable cities, the operators of local railway infrastructures (i.e., metro, light railway, and commuter) are studying strategies to improve the energy efficiency of the overall system. The operators are thus involved in renewing technological infrastructures and examining new operation models for coordinating the motion of the trains fleet. With this regard, the present work proposes a timetable adjustment approach to reduce energy consumption in metro rail transit systems. In addition, a centralized control strategy to manage the output voltage of Traction Power Substations (TPSs), train regenerative power, and charge/discharge power profiles of off-board Energy Storage Systems (ESSs) is proposed. The approach is based on a two-step procedure aimed at optimally allocating the layover time among the train stops. This approach is formulated as an optimization problem, which consider the adopted control strategy, because of the correlation between control actions and timetable. Numerical examples have been carried out based on the real data from metro line 1 of Naples, (Italy). The results highlight the capability of the strategy to achieve relevant results in terms of energy saving. In addition, the advantages introduced by the proposed centralized control strategy are emphasized through a comparison with the conventional local control strategy.**

***Index Terms*—Railway market, energy efficiency, optimal layover time, energy storage system, limited receptivity**

## I. Introduction

NATIONAL network activities are relevant opportunities for the economy. Starting in the early 1990s, the European Commission introduced legislative proposals aimed at liberalizing national monopolistic service markets that hold general economic interests. Also, the railway sector was the object of new legislation addressing both opening the market and rise new financial opportunities [1], [2]. The new era of the railway is based on the separation of the activities, formerly referred to the monopolistic companies, leading to new solutions and economic opportunities. The latter has to be carried out in the paradigm of energy efficiency and sustainability in a sector, where the widespread use of electrical engines and electrical traction enables to provide transportation with no emissions on-site. Moreover, being railways extremely efficient in terms of space required to provide transportation [3], local rail infrastructures represent relevant activities for realizing strategies for sustainable cities.

Metro, commuter, and urban rail systems are also known as local or stopping trains, that operate passenger services inside town or between town and its suburbs. They normally operate with an even service load throughout the day, although there may be a slight increase in services during peak hours, commonly known as rush-hour. Typically, such as in Italy, the local train companies are owned by the region or national rail companies managing the local services under an agreement with the Region. In some areas, it is possible to find a combination of the two. Therefore, the Regional guidelines addressing sustainable urban mobility are frequently designed for forcing Railway System Operators (RSOs) at testing innovative measures for sustainability. These measures typically concern both the renewal of old technologies and the efficient logistic management of the fleets of trains moving on the same tracks. The strategies aim at reducing energy consumption (so improving system sustainability) and thus decreasing the impact on the supply distribution grid.

In this regard, it is worth noting that most of the consumed energy in the railway sector is used for powering trains. Depending on the vehicle, route and weather conditions, the traction energy used to power the vehicle is estimated at around 80%. The rest is used to supply loads in stations and depots [4]. Specifically for the traction energy, Fig. 1 shows a typical distribution of energy flows. Driving energy accounts for the main consumption factor, followed by drive chain losses and onboard auxiliary systems (i.e., lighting, heating, cooling systems and all the services aimed

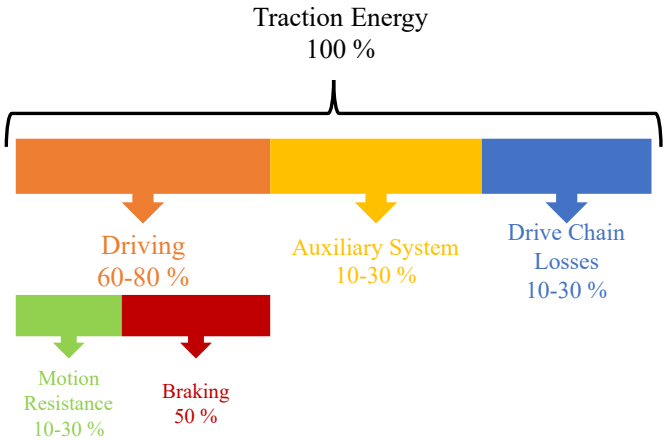


Fig. 1: Typical traction energy flow to power trains.

(corresponding author: Antonio Di Pasquale)
The authors are with the University of Naples Federico II, Italy (e-mail: luca.dacierno@unina.it; marilisa.botte@unina.it; antonio.dipasquale@unina.it; fabio.mottola@unina.it; mario.pagano@unina.it)

at ensuring passenger comfort). Energy consumption can vary considerably depending on the time allowance, time/energy weighting policy and tracking features. Efficiency measures can be applied to railway infrastructure, single or multiple moving rolling stock [5]. In the case of metro and urban applications, the technical literature focused on strategies for efficiency improvements based on proper scheduling of the timetable. It means coordinating the motion of fleets of trains by eco-driving techniques. Eco-driving is the name given to the wide range of train driving techniques intended to reduce both the economic and the environmental impact of train motion. They operate to optimize train speed profiles for reducing traction energy consumption in respect of timetable constraints. They can be used in real-time Driver Advisory Systems (DAS) or Automatic Train Operation (ATO) systems [6]. [7] reported that maximizing the Regenerative Braking (RB) energy exchange between metro trains is the preferential measure to utilize the regenerative energy in urban rail transit.

Timetable optimization is based on eco-driving techniques variously applied to fleets of trains. For instance, early works developed a scheduling algorithm for the design of timetables in order to reduce peak power consumption, avoid oscillations and limit peaks in power demand at the TPSs [8]. In [9], the authors designed a mathematical programming optimization approach based on the synchronization between braking and accelerating trains in the neighbour of passenger stations. Power flow analysis for Madrid metro line 3 showed a 3.5% reduction in energy consumption. [10] used real-world speed profiles for energy estimation and proposed a dwell time control approach to reduce the energy supplied to trains that are in the same electricity supply interval. Similarly in [11], the authors presented an approach based on headway and dwell time adjustments to enhance the use of RB energy. In this regard, [12] developed a bi-objective timetable optimization model to find the optimal timetable with the minimum passenger waiting time and pure energy consumption (i.e., the difference between traction energy and regenerative energy). Numerical simulation for the Beijing Yizhuang metro line pointed out a reduction both in the total energy consumption by 9.67% and in the total passenger waiting time by 4.72% compared with the adopted timetable. Remarkable results were obtained in [13], where the authors proposed a mixed integer linear programming for timetable adjustments. The latter aims at improving the utilization of regenerative energy and shaving power peaks. Indeed, the optimized timetable increases regenerative energy usage by almost 290% and shaves the power peaks by 8.5%. In [14], a modified AC/DC unified power flow algorithm for urban rail traction power supply systems with energy feedback systems is proposed. Numerical results disclosed that this approach allows achieving remarkable results like 11% energy saving. The authors pointed out that these results depend on the system operating voltage. Single-criteria and multiple-criteria mixed integer approaches can be formulated.

This paper proposes a timetable adjustment strategy for a fleet of metro trains that is aimed at improving the energy efficiency of the system by recovering RB energy. A control strategy based on an optimal power flow approach for a smart traction system is proposed. The smart paradigm is applied by using a control strategy based on exchanging data among the trains and electrical equipment of the traction infrastructure. Compared to the mode of operating of the conventional traction systems, in which TPSs adopt local control, the proposed strategy allows for obtaining: i) proper management of the power flow, ii) effective control of the voltage along the traction lines. The strategy proposed in this work requires a centralized supervisor that regulates the TPS output voltage and manages both the charging/discharging of ESSs installed in the substations of TPSs and the power coming from the RB. The optimal power flow is formulated as an optimization problem aimed at minimizing train voltage deviations around the nominal value and maximizing energy savings. The main contribution of this paper refers to a comprehensive approach that simultaneously accounts for the optimal fleet timetable design while applying operation measures typically applied for efficiency improvements. These measures refer to voltage profile optimization and the reduction of energy consumption by exploiting RB. Finally, the effectiveness of the proposed approach is validated by numerical simulations considering the metro line 1 of Naples (Italy). Comparisons of the proposed centralized approach with the local control strategy are reported and discussed. In both cases, the role of ESSs installed at the TPSs and the advantages obtained by their use are discussed in terms of both voltage profile and energy efficiency improvements.

The rest of the paper is organized as follows. Section II gives the main relevant notes on railway metro systems. Section III provides some theoretical fundamentals for the electrical analysis of the traction system. Section IV briefly discusses about the layover-time definition for a cyclical service. In Section V a two-steps procedure to optimally allocate layover time and manage power flows in the DC network is presented. In Section VI the results of numerical analysis focusing on the real case study of metro line 1 of Naples are shown. In Section VII the remarkable notes are highlighted.

## II. DC Electric Railway Traction System Modeling

Fig. 2 shows a typical configuration of a DC railway traction system. The supply network consists of TPSs located throughout the track, two overhead contact lines (i.e., one for each direction), and running rails. TPSs are, typically, fed by the AC distribution grid using a three-phase transformer with a single or double secondary winding, to which one or two diode bridge rectifiers are connected. On-load tap-changers, connected to the transformers via tap winding, allow regulating

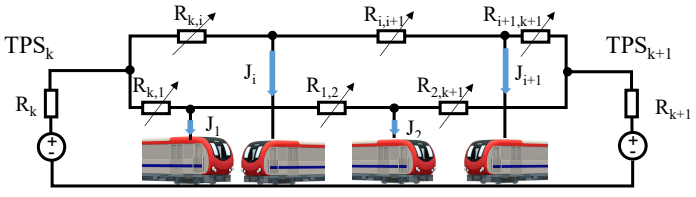


Fig. 2: Representative scheme of an urban DC traction system.

the output voltage, which is then smoothed by an LC low-pass filter. Hence, substations are modelled by a real DC voltage source, i.e., an ideal voltage source $\mathbf{V}_{\text{TPS}_\text{k}}$ with in series an equivalent resistance $R_\text{k}$, which accounts for the linearized characteristic of the diode bridge. Trains collect their current from overhead contact lines by the pantograph, whereas running rails provide a return path for the traction currents. Thus, the traction circuit is modeled by equivalent resistances, which depend on the position of trains and are calculated according to the per-unit of length resistance values of contact wires and rails. A more detailed explanation is provided in [15]. Trains are modeled as controllable DC current source $J_\text{j}$, whose value is given by (the dependence on the time is not reported for clarity):

$$J_\text{j} = \frac{P_\text{el,j}}{V_\text{i}} \tag{1}$$

where $P_\text{el,j}$ and $V_\text{j}$ are the power demand and the supply voltage of the i-th train, respectively. The total train electrical power is given by

$$P_\text{el,j} = P_\text{aux} + \gamma \cdot P_\text{m} \tag{2}$$

where $P_\text{aux}$ is the power spent to supply the train auxiliary systems (e.g., lightning, cooling systems, etc.), whereas $\gamma$ is the electro-mechanical efficiency, which accounts for the conversion of electrical power into mechanical power ($P_\text{m}$) and vice versa. Therefore, $\gamma$ may assume two different expression according to the sign of $P_\text{m}$

$$\gamma = \begin{cases} 1/\eta_{tr} & \text{if} \quad P_\text{m} > 0 \\ \eta_{br} & \text{if} \quad P_\text{m} < 0 \end{cases} \tag{3}$$

where $\eta_{tr}$ accounts for the conversion efficiency of electrical power into mechanical one, whereas $\eta_{br}$ accounts for the conversion efficiency of kinetic energy into electricity by RB. It has to be noted that trains can perform blended braking, i.e., the combination of rheostatic and RB, and only the power coming from the latter may be saved. $P_\text{m}$ represents the mechanical power required for the motion of the train and it depends on the resistance forces as follows

$$P_\text{m} = v\left(R(v) + M_\text{eq}\frac{d}{dt}v\right) \tag{4}$$

where $v$ is the speed of the train, $M_\text{eq}$ is the equivalent mass of the train accounting also the effects of rotating masses and $R$ is the resultant of the aerodynamic resistances and the resistance forces due to the curvature radius and the slope of the track. A suitable expression for all these quantities can be found in [16].

Concerning (4), once all the features of the track are known, two possible approaches can be applied:

- backward approach: the speed is assigned to calculate the mechanical power and all the features of the train motion;
- forward approach: the traction force or the power are assigned to calculate the speed and all the features of the train motion [17].

This study adopts the backward approach. Indeed, the proposed procedure aims at optimally managing the railway system when the feature of the service, in terms of train speed profile, is assigned.

## III. Traction Power Flow

In this section, some theoretical fundamentals for the steady-state electrical analysis of the railway traction system are recalled. The aim of the analysis is to determine the supply voltage for each train and the power supplied by each substation.

Consider a generic electric traction system modeled as explained in Section II. Let $n_\text{L} \in \mathbb{N}$ be the number of load buses, namely the nodes in which trains are connected and the connection nodes between branches, $n_\text{TPS} \in \mathbb{N}$ the number of TPSs, and $n = n_\text{L} + n_\text{TPS}$ the total number of nodes. The power flow equations for the system under study can be written in the following matrix form:

$$\text{diag}\{\mathbf{V}\} \cdot \mathbf{G} \cdot \mathbf{V} = \mathbf{P} \tag{5}$$

where the operator *diag* gives a diagonal matrix, $\mathbf{V} \in \mathbb{R}^n$ is the vector of nodal voltages, $\mathbf{G} \in \mathbb{R}^{n \times n}$ is the conductance matrix and $\mathbf{P} \in \mathbb{R}^n$ is the vector of injected powers. The above-mentioned quantities can be expressed in *per unit* with respect to a base $\mathcal{B} = \{V_\text{b}, G_\text{b}, P_\text{b}\}$, where $V_\text{b}$, $G_\text{b}$ and $P_\text{b}$ represent reference values for voltage, conductance and power, respectively. For the sake of clarity, (5) can be rewritten as:

$$\text{diag}\left\{\begin{bmatrix} \mathbf{V}_\text{TPS} \\ \mathbf{V}_\text{L} \end{bmatrix}\right\} \begin{bmatrix} \mathbf{G}_{11} & \mathbf{G}_{12} \\ \mathbf{G}_{21} & \mathbf{G}_{22} \end{bmatrix} \begin{bmatrix} \mathbf{V}_\text{TPS} \\ \mathbf{V}_\text{L} \end{bmatrix} = \begin{bmatrix} \mathbf{P}_\text{TPS} \\ \mathbf{P}_\text{L} \end{bmatrix} \tag{6}$$

where $\mathbf{V}_\text{TPS} \in \mathbb{R}^{n_\text{TPS}}$ and $\mathbf{P}_\text{TPS} \in \mathbb{R}^{n_\text{TPS}}$ are the nodal voltage and injected power vectors of TPSs, whereas $\mathbf{V}_\text{L} \in \mathbb{R}^{n_\text{L}}$ and $\mathbf{P}_\text{L} \in \mathbb{R}^{n_\text{L}}$ are the nodal voltage and injected power vectors of load buses, $\mathbf{G}_{11} \in \mathbb{R}^{n_\text{TPS} \times n_\text{TPS}}$, $\mathbf{G}_{22} \in \mathbb{R}^{n_\text{L} \times n_\text{L}}$, $\mathbf{G}_{12} \in \mathbb{R}^{n_\text{TPS} \times n_\text{L}}$ and $\mathbf{G}_{21} \in \mathbb{R}^{n_\text{L} \times n_\text{TPS}}$ are the sub-matrices of the nodal conductance matrix. It has to be noted that the terms of $\mathbf{G}$ need to be updated according to the trains position since trains' motion dynamically changes the topology of the network. With regard to (6), typically $\mathbf{P}_\text{TPS}$ and $\mathbf{V}_\text{L}$ are the unknown variables, whereas $\mathbf{V}_\text{TPS}$ and $\mathbf{P}_\text{L}$ are known. In more detail, being $\mathcal{T}$ the subset of nodes in which trains are connected, the components $P_\text{L,j}$ of $\mathbf{P}_\text{L}$ can be assigned as follows

$$P_\text{L,j} = \begin{cases} -P_\text{el,j} & \text{if j} \in \mathcal{T} \\ 0 & \text{otherwise.} \end{cases} \tag{7}$$

The terms of $\mathbf{V}_\text{TPS}$ may vary according to the the turn ratio selected by the tap-changers, which are usually controlled through a local control strategy.

## IV. Layover time

As shown in the recent literature [18], a frequency-based system may be modelled as a cyclical service, as described in Figs. 3 and 4. The main parameter of a cyclical service model is the minimum cycle time ($CT_\text{min}$) which represents the time required by a train:

- to perform the outward trip,
- to be prepared at the first terminal station for the subsequent trip,
- to perform the return trip,
- to be prepared at the second terminal station for the subsequent trip.

This article has been accepted for publication in IEEE Transactions on Vehicular Technology. This is the author's version which has not been fully edited and content may change prior to final publication. Citation information: DOI 10.1109/TVT.2024.3353348



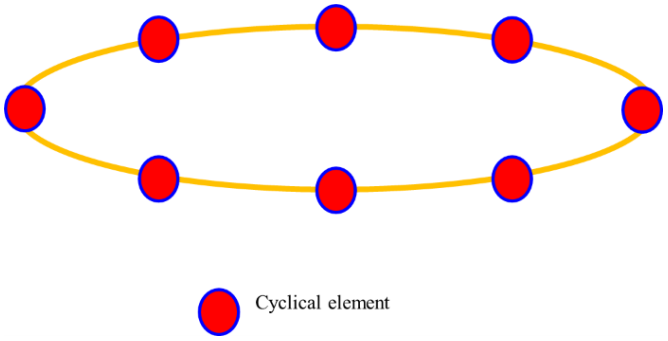


Fig. 3: Scheme of cyclical service.

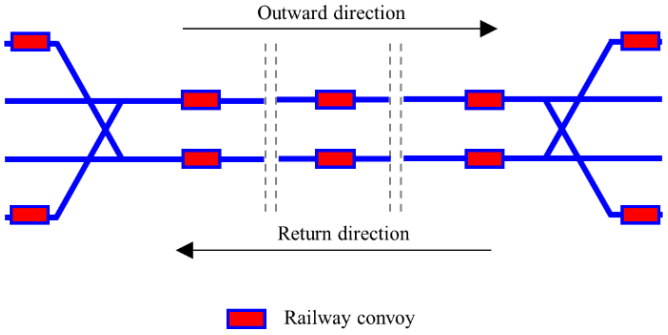


Fig. 4: Representation of a railway service

The value of $CT_{\text{min}}$ can be calculated as:

$$CT_{\text{min}} = \sum_{lot} RT_{lot} + \sum_{sot} DT_{sot} + lT_{ot} + ST_{ot} + \\ + \sum_{lrt} RT_{lrt} + \sum_{srt} DT_{srt} + lT_{rt} + ST_{rt} \tag{8}$$

where $RT_{lot}$ and $RT_{lrt}$ the running times spent by a train travelling on link $l$ between two subsequent stations during the outward (*ot*) and return (*rt*) trip, respectively; $DT_{sot}$ and $DT_{srt}$ are the dwell time spent by a train in a stop condition at the station $s$ during the *ot* and *rt* trip, respectively; ($lT_{sot}$) and ($lT_{srt}$) the inversion time spent by a train at the terminal station of the *ot* and *rt*, respectively, both to be prepared for the subsequent trip; $ST_{ot}$ and $ST_{rt}$ the supplement time spent by a train at the terminal station of the *ot* and *rt*, respectively, for compensating primary and secondary delays. The minimum number of rail convoys ($N_{\text{RC}}$) to perform the service with a prefixed planned headway ($\text{H}_{\text{plan}}$) be calculated as:

$$N_{\text{RC}} = \text{floor}\left(\frac{CT_{\text{min}}}{\text{H}_{\text{plan}}}\right) + 1 \tag{9}$$

where floor operator rounds the argument to the nearest integer less than or equal to that element.

A perfect cyclical service, performed by a number of vehicles equal to $N_{\text{RC}}$, with a time spacing equal to $\text{H}_{\text{plan}}$, requires a planned cycle time ($CT_{\text{plan}}$) calculated as:

$$CT_{\text{plan}} = N_{\text{RC}} \cdot \text{H}_{\text{plan}} \tag{10}$$

In that regard, it is necessary to consider a further time, the total layover time ($LT_{\text{tot}}$), which allows performing the considered railway service according to the cyclical paradigm. Hence, $LT_{\text{tot}}$ can be calculated as follows:

$$LT_{\text{tot}} = CT_{\text{plan}} - CT_{\text{min}} \tag{11}$$

where the total layover time represents the time spent by the train in a stop condition by waiting for the planned departure time. Obviously, the layover time may be allocated differently thought the stations of the line (e.g., entirely at the first station, entirely at the last station, equally distributed among the intermediate stations, etc.) so that the sum of layover times in each station would be equal to $LT_{\text{tot}}$.

The adoption of a cyclical paradigm, with the assumption of homogeneous fleet composition, allows adopting a simulation period equal to the planned headway ($CT_{\text{plan}}$) since the service recurs with equal features (i.e., the only difference is that the first convoy will occupy the position of the second, the second that of the third, and so on).

## V. Two-Step Optimization Procedure for Smart Traction Systems

This section presents the two-step optimal procedure used to allocate layover time for metro railway applications. Such a procedure is based on:

i. the evaluation of the decisions taken by the control strategy adopted by the railway system. (For instance, in the following a new centralized optimal control strategy, which is aimed at both minimizing the train voltage deviations around the nominal value and maximizing the saved energy from RB, will be considered);
ii. the optimal allocation of the layover time, which provides the fleet timetable coherent with the goals of the adopted control strategy.

Hence, the proposed approach carries out the optimization of the timetable in terms of layover time (step 2) by taking into account the results of the adopted control strategy of (step 1). Indeed, the optimal adjustment of the timetable cannot be addressed without considering the actions of the adopted control strategy because of their correlation.

### A. Centralized Optimal Control Strategy

Typically, DC railway systems adopt a local control strategy, which aims to regulate the substation voltages and take the train voltage values within an acceptable range. Indeed, trains implement an on-board squeeze control according to which power injection (or absorption) is reduced if the catenary voltage of any train exceeds the prescribed limits [19]. The absence of coordination among control actions does not allow effective management of the power flows in the traction network and affects the capability of the system to save energy. On the contrary, centralized control strategies aim at regulating train voltages [20], thus allowing an effective managing of the power flows along the lines. To be applied, they require a smart system, where an information exchanging platform, through which a Central Controller communicates with trains, TPSs, and ESSs, is needed. A schematic representation of a smart traction system is shown in Fig. 5. The Central Controller elaborates data (e.g., train position and power requirements,

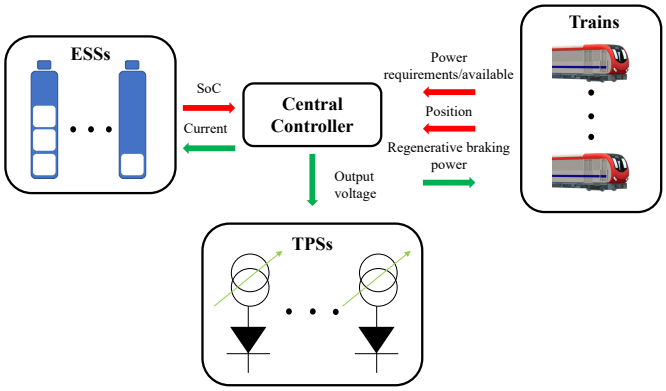


Fig. 5: Structure of a centralized control system. The central controller exchanges information (i.e., input (red) and output (green)) with trains, ESSs and TPSs.

ESSs SoC) and sends voltage setpoints to all the TPSs and power setpoints to each ESS and train.

In particular, herein it is proposed a centralized control strategy conceived for already existing traction systems, which typically feature uncontrolled AC/DC converters. Therefore, in order to exploit the train RB, it is assumed that at each TPS an ESS is installed. This choice, as pointed out in [21], is motivated by the fact that, even if reversible substations are preferred in terms of energy efficiency, they are not able to reduce power peaks, which are main responsible of the energy losses in the traction systems. Therefore, the installation of ESSs at the TPSs represents the most effective measure for reducing power peaks, which do not depend so much on reducing the power peaks of each train independently, but on reducing the peak consumption in the TPSs.

In order to use the proposed strategy within the second step, a scheduling procedure should be implemented which aims at both regulating train voltages and recovering as much power from RB as possible, which contemporaneously accounts for all time intervals included in the planning time horizon. This scheduling procedure is formulated as an optimal power flow problem, whose objective function to minimize is:

$$f_{\text{obj,cs}} = \sum_{k=1}^{\text{H}_{\text{plan}}} f_{\text{obj,cs}}^{(k)} = \sum_{k=1}^{\text{H}_{\text{plan}}} \Big[ (\mathbb{1} - \mathbf{V}_{\text{L}}^{(k)})^{\text{T}} (\mathbb{1} - \mathbf{V}_{\text{L}}^{(k)}) + \\ + (\mathbb{1} - \boldsymbol{\alpha}^{(k)})^{\text{T}} (\mathbb{1} - \boldsymbol{\alpha}^{(k)}) \Big] \tag{12}$$

where, $\mathbb{1} \in \mathbb{R}^{n_{\text{L}}}$ is the unity vector, $\mathbf{V}_{\text{L}}^{(k)}$ is expressed in pu, $\text{H}_{\text{plan}}$ is the time horizon considered since the service features are periodical with a period equals to the headway value, and $\boldsymbol{\alpha}^{(k)} \in \mathbb{R}^{n_{\text{L}}}$ is a vector of values in the range $[0, 1]$ whose components are defined as [22]:

$$\alpha_{\text{j}}^{(k)} = \begin{cases} \dfrac{P_{\text{rec,j}}^{(k)}}{P_{\text{L,j}}^{(k)}} & \text{if } P_{\text{L,j}}^{(k)} > 0 \\ 1 & \text{otherwise} \end{cases} \tag{13}$$

where $P_{\text{rec,j}}^{(k)}$ is the recovered power from the RB of the j-th train. For instance, during the braking phase, if $\alpha_{\text{j}}^{(k)} = 0$ means that the j-th train will perform a full rheostatic braking, on the contrary if $\alpha_{\text{j}}^{(k)} = 1$ means that all the power available during the braking will be recovered. Thus, the optimization problem seeks to minimize the squared error of nodal voltages with respect to the reference values while maximizing the recovered power from RB by minimizing the squared error of $\boldsymbol{\alpha}$ with respect to the desired value (i.e., $\mathbb{1}$). The problem is subject to a set of linear and non linear constraints referring to nodal voltages and injected powers as reported below

$$\mathbf{V}_{\text{min}} \leq \mathbf{V}^{(k)} \leq \mathbf{V}_{\text{max}} \tag{14}$$

$$\mathbf{P}_{\text{min}} \leq \mathbf{P}_{\text{TPS}}^{(k)} \leq \mathbf{P}_{\text{max}} \tag{15}$$

$$\mathbf{P}_{\text{L}}^{(k)} = \text{diag}\{\boldsymbol{\alpha}^{(k)}\} \mathbf{P}_{\text{L}}^{(k)*} \tag{16}$$

Constraints (14)-(16) apply for all time interval $k = 1, 2, \ldots, \text{H}_{\text{plan}}$. The linear constraint (14) limits nodal voltages in an acceptable range, in particular $\mathbf{V}_{\text{min}} \in \mathbb{R}^{n_{\text{L}}}$ and $\mathbf{V}_{\text{max}} \in \mathbb{R}^{n_{\text{L}}}$ take into account the limited TPSs range of voltage regulation and the limitation prescribed by the Standard EN 50163 [23]. Indeed, the latter admits voltage variation $[-30\%, +20\%]$ around the nominal voltage value of the system. The nonlinear inequality constraint (15) limits the maximum power supplied by each TPS to its rated value $\mathbf{P}_{\text{max}}$, and $\mathbf{P}_{\text{min}}$ ($\leq 0$) is related to the maximum power that can be absorbed at the TPSs. According to the power flow model reported in (6), constraint (15) can be rewritten as:

$$\mathbf{P}_{\text{min}} \leq \text{diag}\{\mathbf{V}_{\text{TPS}}^{(k)}\} \left[ \mathbf{G}_{11}^{(k)} \mathbf{V}_{\text{TPS}}^{(k)} + \mathbf{G}_{12}^{(k)} \mathbf{V}_{\text{L}}^{(k)} \right] \leq \mathbf{P}_{\text{max}} \tag{17}$$

The nonlinear equality constraint (16) assigns the value of power injected in the load buses as highlighted by (7). It can be rewritten as follows

$$\text{diag}\{\mathbf{V}_{\text{L}}^{(k)}\} \left[ \mathbf{G}_{21}^{(k)} \mathbf{V}_{\text{TPS}}^{(k)} + \mathbf{G}_{22}^{(k)} \mathbf{V}_{\text{L}}^{(k)} \right] = \text{diag}\{\boldsymbol{\alpha}^{(k)}\} \mathbf{P}_{\text{L}}^{(k)*} \tag{18}$$

Regarding the ESSs, their state of charge must be bounded by the minimum and maximum values:

$$\text{SoC}_{\text{j,min}} \leq \text{SoC}_{\text{j}}^{(k)} \leq \text{SoC}_{\text{j,max}} \tag{19}$$

where $\text{SoC}_{\text{j}}^{(k)} \in \mathbb{R}^{n_{\text{ESS}}}$ is the vector containing the state of charge of the j-th ESS ($\text{j} = 1, \ldots, n_{\text{ESS}}$) at time interval $k$. In addition, according to the cyclical nature of the railway service, it needs to ensure that the initial and final values of SoC coincide, therefore:

$$\text{SoC}_{\text{j}}^{(0)} = \text{SoC}_{\text{j}}^{(\text{H}_{\text{plan}})} \tag{20}$$

The state of charge of the j-th ESS is computed according to [24]:

$$\text{SoC}_{\text{j}}^{(k+1)} = \text{SoC}_{\text{j}}^{(k)} - \frac{\Delta T}{C_{\text{j}}} \left( \frac{1}{\eta_{\text{dis}}} P_{\text{ESS,dis,j}}^{(k)} + \eta_{\text{ch}} P_{\text{ESS,ch,j}}^{(k)} \right) \tag{21}$$

where $C_{\text{j}}$ is the battery capacity, $P_{\text{ESS,dis,j}}^{(k)}$ ($\geq 0$) is the ESS charging power, $\eta_{\text{dis}}$ is its charging efficiency, $P_{\text{ESS,ch,j}}^{(k)}$ ($\leq 0$) is the ESS discharging power, and $\eta_{\text{ch}}$ is its discharging efficiency. Obviously, the following expression must be satisfied:

$$P_{\text{ESS,dis,j}}^{(k)} \cdot P_{\text{ESS,ch,j}}^{(k)} = 0 \quad \forall\, \text{j}, k \tag{22}$$

Thus, the optimal power flow aims at finding the optimal values of $\mathbf{V}_{\text{TPS}}$, $\boldsymbol{\alpha}$ and ESSs charging/discharging power

profiles that make the supply voltage profile as smooth as possible and allow recovering as much power from trains RB as possible. This optimization problem can be summarized as follows:

$$\text{OPF}(LT) = \begin{cases} \mathbf{x}_{\text{opt}} = \arg\min \{f_{\text{obj,cs}}(\mathbf{x})\} \\ \text{s.t.} \\ \text{(14), (17), (18), (19), (20), (21) and (22)} \end{cases} \tag{23}$$

where

$$\mathbf{x} = [\mathbf{V}_{\text{TPS}}, \boldsymbol{\alpha}, \text{SoC}, \mathbf{P}_{\text{ESS,dis}}, \mathbf{P}_{\text{ESS,ch}}] \tag{24}$$

It has to be highlighted that in the optimal power flow model the dependence on layover time ($\mathbf{LT} \in \mathbb{R}^{n_{\text{stop}}}$) is enclosed in $\mathbf{G}$ and $\mathbf{P}_{\text{L}}^{*}$ since different configurations of layover determine variations in the train position and their power requirements over time.

### B. Optimal Allocation of Layover Time

Different allocations of layover times thought the stations of the line provide different temporal offsets among motion phased of rail trains. As a consequence, different configurations of layover times may imply different power and energy requirements at the TPSs.

This section presents a method to optimally allocate layover time when the optimal centralized control strategy explained in the previous section is adopted. The problem is formulated as a constrained minimization problem that aims to minimize the overall energy supplied by the TPSs, therefore the objective function to minimize can be written as follows

$$f_{\text{obj,lt}} = \sum_{q=1}^{n_{\text{TPS}}} \sum_{k=1}^{k_{\text{end}}} P_{\text{TPS},q}^{(k)} \cdot \Delta T \tag{25}$$

where $k_{\text{end}} = \text{H}_{\text{plan}}/\Delta T$ with $\Delta T$ sampled time. Indeed, being all the features of the service (e.g., power demands, speed profiles, etc.) periodical with a period equal to the headway, the analysis can be performed on the restricted time horizon of amplitude equal to $\text{H}_{\text{plan}}$. Moreover, the following constrains apply

$$LT_s \geq 0 \quad \forall j \tag{26}$$

$$\sum_{s=1}^{n_{\text{stop}}} LT_s = LT_{\text{tot}} \tag{27}$$

When both passenger running and waiting times are desired to be kept constant, it is possible to allocate all layover times at terminal stations. Hence, the constraint (27) can be modified as follows where (26) expresses that the layover times allocated at any station have to be non-negative values, whereas (27) imposes that the sum of layover times allocated at any station has to be equal to the total layover time ($LT_{\text{tot}}$).

$$LT_1 + LT_2 = LT_{\text{tot}} \tag{28}$$

where $LT_1$ and $LT_2$ represent the time allocated at the two terminal stations.

In this case, allocating the layover time only at the terminals means changing the departure time of the first trip of the outward trip and the departure time of the second trip of the return trip. Obviously, since the service has been modelled as frequency-based, a different departure time for the first trips (however, it is only a few seconds) does not generate variations in the service quality from a passenger perspective.

Thus, the procedure leading to find the optimal value of $LT$ can be summarized as follows

$$\begin{cases} \mathbf{LT}_{\text{opt}} = \arg\min_{\mathbf{LT}} \{f_{\text{obj,lt}}(\mathbf{LT}, \mathbf{x})\} \\ \text{s.t.} \\ \text{(26) and (28)} \\ \text{OPF}(\mathbf{LT}) \end{cases} \tag{29}$$

Concerning (29), it is reasonable narrowing the set of admissible value for $LT$ to the set of natural numbers, i.e., $LT_1$ and $LT_2$ are assigned as integer multiples of 1 s including the zero. According to this assumption, the problem can be addressed through an exhaustive approach. Indeed the number of possible pairs $(LT_1, LT_2)$ is equal to $LT_{\text{tot}} + 1$.

Thus, in order to solve (29) the optimal power flow problem (23) is solved for each pair $(LT_1, LT_2)$ on the entire time horizon ($\text{H}_{\text{plan}}$) and then the pair providing the lowest value of $f_{\text{obj,lt}}$ is selected as solution, as described in Algorithm 1.

**Algorithm 1** Two-step Procedure

**for** $LT_1 \leftarrow 1, LT_{\text{tot}}$ **do**
  $LT_2 \leftarrow LT_{\text{tot}} - LT_1$
  $\mathbf{G} \leftarrow \mathbf{G}(LT_1, LT_2)$
  $\mathbf{P}_{\text{L}} \leftarrow \mathbf{P}_{\text{L}}(LT_1, LT_2)$
  # Step 1
  $(\mathbf{V}_{\text{TPS,opt}}, \boldsymbol{\alpha}_{\text{opt}}) \leftarrow$ OPF ▷ Eq. (23)
  $\mathbf{P}_{\text{TPS,opt}} \leftarrow \mathbf{P}_{\text{TPS}}(\mathbf{V}_{\text{TPS,opt}}, \boldsymbol{\alpha}_{\text{opt}})$ ▷ Eq. (6)
  Compute (25)
**end for**
# Step 2
find $\mathbf{LT}_{\text{opt}}$ that minimize (25)

## VI. Numerical Analysis

The numerical analysis focuses on the real case of metro line 1 of Naples (Italy). As reported in Table I, the metro track is about 18 km long including 19 stops. Trains are fed

TABLE I: Main System parameters

| Description | Symbol | Value |
|---|---|---|
| Equivalent train mass | $\text{M}_{\text{train,eq}}$ | $158 \cdot 10^3$ kg |
| Train traction efficiency | $\eta_{\text{Tr}}$ | 0.9 |
| Train braking efficiency | $\eta_{\text{Br}}$ | 0.85 |
| Route length | $\text{L}_{\text{route}}$ | 18 km |
| Number of TPS | $\text{N}_{\text{TPS}}$ | 7 |
| Number of stations | $\text{N}_{\text{stop}}$ | 19 |
| Number of trains | $n_{\text{train}}$ | 26 |
| Travel time (outward + return) | $\text{T}_{\text{trip}}$ | 4542 s |
| Headway | $\text{H}_{\text{plan}}$ | 180 s |
| Layover time | $LT$ | 138 s |
| Rated voltage | $\text{V}_{\text{n}}$ | 1500 V |
| TPS maximum power | $\text{P}_{\text{TPS,max}}$ | 7 MW |
| Resistence per unit of length | r | 0.03 Ω/km |
| TPS equivalent resistence | $\text{R}_{\text{TPS}}$ | 0.03 Ω |

by a 1500 V DC traction circuit, which features 7 TPSs with a rated power of 7 MW. According to the data reported in Table I the power, speed and space profiles of the moving trains are determined by the well-know railway simulation software *OpenTrack*. It has to be noted that a headway of 3 min was assumed, indeed, although currently the service is performed according to a value of 9 min, the former represents the reference value adopted in the design stage of the railway system. This means that the metro service features are periodical with a period equal to 3 min. Therefore, the latter represents a suitable observation window to perform the analysis of the system under examination.

In order to highlight the effectiveness of the proposed strategy and the cross dependence between timetable adjustments/design and control strategy adopted by the railway system, the following three scenarios are analysed, which refer to the optimal allocation of the layover time carried out according to:

- *Case A*: the conventional local control without storage systems;
- *Case B*: the conventional local control with a storage system installed at each TPS;
- *Case C*: the proposed centralized control strategy with a storage system installed at each TPS.

Case A and Case B adopt the conventional local control strategy. The evaluation of the energy consumption is tackled through a power flow problem which takes into account the limited network receptivity [25] (*see* Appendix A for further details). Case C adopts the two-step optimization procedure presented in Section V, relying on the centralized control strategy.

According to the metro cyclical service, the layover time $LT_{\text{tot}}$, which has to be comprehensively assigned at the two terminal stations, is 138 s. The two-step optimization procedure aims at assigning the above-mentioned layover time s.t. $LT_1 + LT_2 = 138$ s, where $LT_1$ is the layover time assigned at the terminal station 1 and $LT_2$ is the layover time assigned at the terminal station 2 (i.e., the terminal stations of the outward and return trips). Fig. 6 shows how the allocation of layover time affects the timetable. It can be noted how the assignment of non-zero optimal layover time (i.e., $LT_1^* \neq 0$) delays the departure of the train during the return trip.

The following subsections show the results of the considered three scenarios in terms of both energy consumption and voltage regulation.

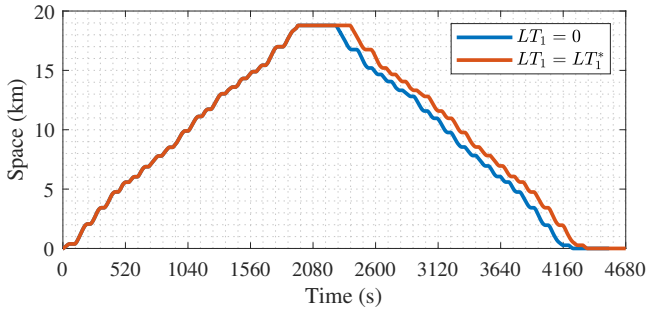


Fig. 6: Space vs time for $LT_1 = 0$ s and $LT_1 = LT_1^*$.

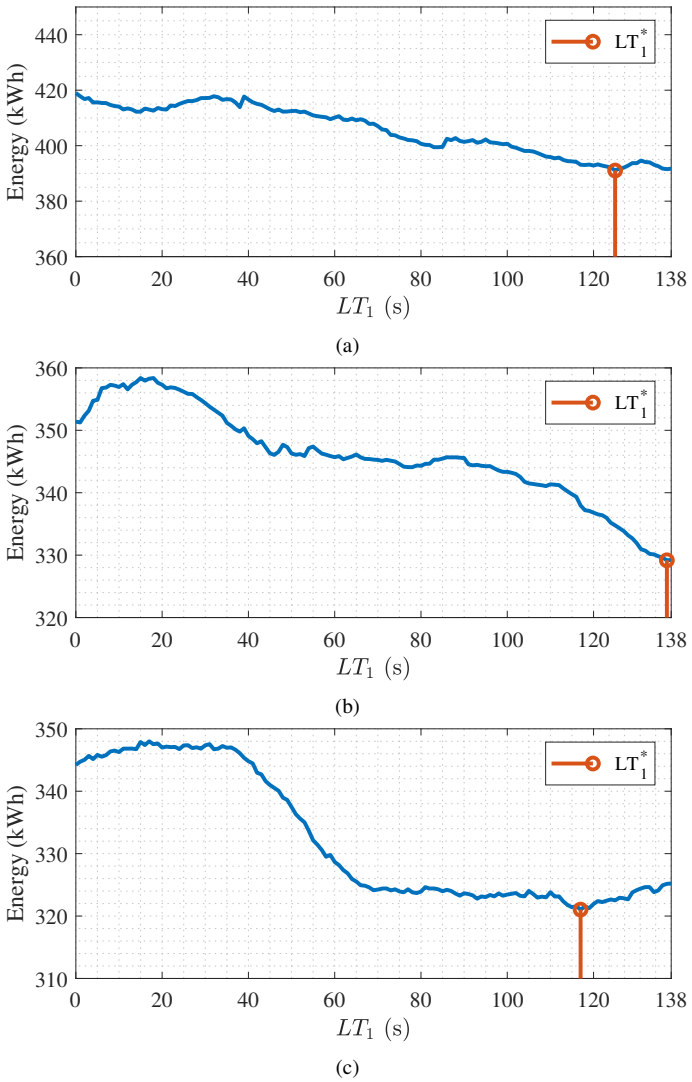


Fig. 7: Energy supplied by the entire electric traction system for all the values of $LT_1$ and in red the value minimizing energy consumption for Case A (a), Case B (b) and Case C (c).

### A. Comparison in terms of energy consumption

Fig. 7 shows the energy consumption of the traction system for all the possible allocations of the layover time in the three case studies. The red circle markers indicate the optimal values for $LT_1$, which represent the solutions corresponding to the lowest value of energy consumption. It should be noted that the optimal value of $LT_1$ depends on the adopted control strategy and the features of the system, including the presence of the storage. In Case A the value of $LT_1^* = 125$ s leads to a 6.70% reduction in energy consumption compared to the worst allocation of layover time. In Case B the optimal allocation of the layover time consists in choosing $LT_1^* = 137$ s, resulting approximately in 8% of energy saving. Regarding Case C, the value of $LT_1^* = 117$ s is obtained, which leads to a 7.75% reduction in energy consumption compared to the worst allocation of layover time. The comparison of these results is better highlighted in Table II. The table clearly shows that, regardless of the nature of the control, the optimal allocation of layover time is able to provide almost a 7-8% reduction in

energy consumption if compared with the worst allocation of layover time. In addition, compared to Case A, the use of the storage systems allows for saving more than 15% of energy in the presence of the local control strategy (Case B) and almost 18% in the case of the proposed centralized control strategy (Case C).

Fig. 8 shows the amount of saved energy and the energy losses for all the possible values of $LT_1$ in the three case studies. Specifically, the blue lines refer to the saved energy by RB, whereas the red lines represent the energy dissipated by the supply traction system. The total amount of energy available during the RB is approximately 173 kWh, which is completely recovered in Case C regardless of the allocation of layover time. In contrast, due to the limited receptivity of the network, Case A and Case B present lower saved energy from RB, which varies between 34-47% and between 66-79%, respectively, depending on $LT_1$. It is important to note that storage systems play a crucial role in enhancing the receptivity of the network and enabling a higher amount of energy to be saved from RB. Additionally, the proposed centralized control strategy further enhances the receptivity of the network, ultimately leading to the complete saving of all the energy generated during the RB. With this regard, Fig. 8 shows how both energy losses and regenerative energy vary with respect to the allocation of the layover time. Remarkably, in Case C, being the amount of saved energy from RB constant, the optimal value of $LT_1$ coincides with the solution providing the lowest value of energy losses. Moreover, it is interesting to note that both Case A and Case B, compared to Case C, exhibit lower energy losses. Indeed, as explained in the following, the local control strategy increases the catenary's voltage, resulting in reduced currents.

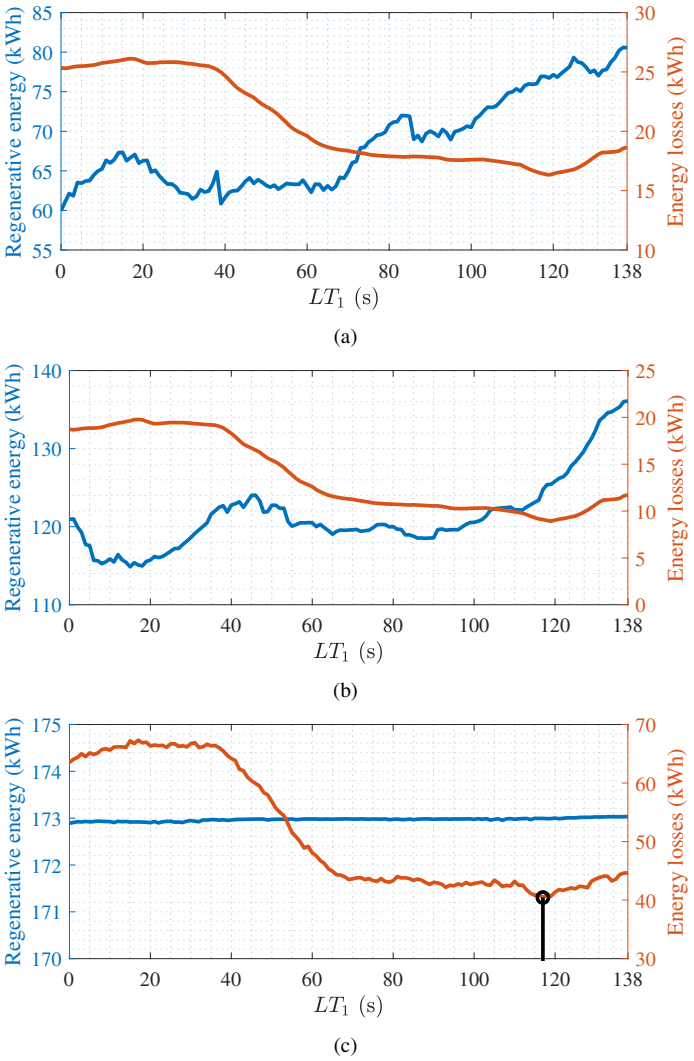


Fig. 8: Regenerative energy (blu) and energy losses (red) over $LT_1$, for Case A (a), Case B (b) and Case C (c). In the latter, $LT_1^* = 117$ coincides with the value of $LT_1$ (marked with black) providing the minimum value of energy losses.

### B. Comparison in terms of Voltage Regulation

In order to evaluate the performances of the control strategies in terms of voltage regulation, the mean square error, $S_V$, is used:

$$S_V = \sqrt{\frac{1}{n_{L \cdot H_{plan}}} \sum_{j=1}^{n_L} \sum_{k=1}^{H_{plan}} \left( V_{ref} - V_{L,j}^{(k)} \right)^2} \qquad (30)$$

which is evaluated with respect to the reference value (e.g., $V_{ref} = 1$ pu) for the train voltages over the entire time horizon.

Fig. 9 shows the values assumed by the index for all the values of $LT_1$.It points out that the proposed centralized control strategy, compared with the local one, allows for more effective voltage regulation. Indeed, Fig. 9c exhibits values of $S_V$ significantly lower than Fig. 9a-9b. Moreover, the local control does not provide effective regulation of the catenary voltage. This reduces the receptivity of the system, leading trains to reduce regenerative power in order to bring the voltage values within the prescribed limits. This determines trains' voltages close to the over-voltage limit (i.e., 1.2 pu). It has to be highlighted that in Case A the energy recovered by RB is due only to the power exchanges among braking and moving trains as long as the voltage does not exceed the limits. In Case B the storage system's control aims at regulating the local voltage (*see* Appendix B for further details), this results in charging the storage when the voltage is higher than the upper limit, and discharging it when the voltage is lower than the lower limit. As shown in Fig. 9b, beyond saving more regenerative energy, the employment of storage systems enhances the regulation of the trains' voltages. Finally, the centralized proposed strategy, by coordinating the operations among storage systems, trains and TPSs, allows for the optimal regulation of the trains' voltages.

TABLE II: Energy Consumption Comparisons and Percentage Reduction Compared to Case A

| Case | Worst $LT_1$ (s) | $LT_1^*$ (s) | Energy (kWh) Worst | Energy (kWh) Best | $\Delta E$ (%) |
|---|---|---|---|---|---|
| A | 0 | 125 | 419 | 391 | (-) |
| B | 18 | 137 | 358 | 329 | (-15.8) |
| C | 17 | 117 | 350 | 321 | (-17.9) |

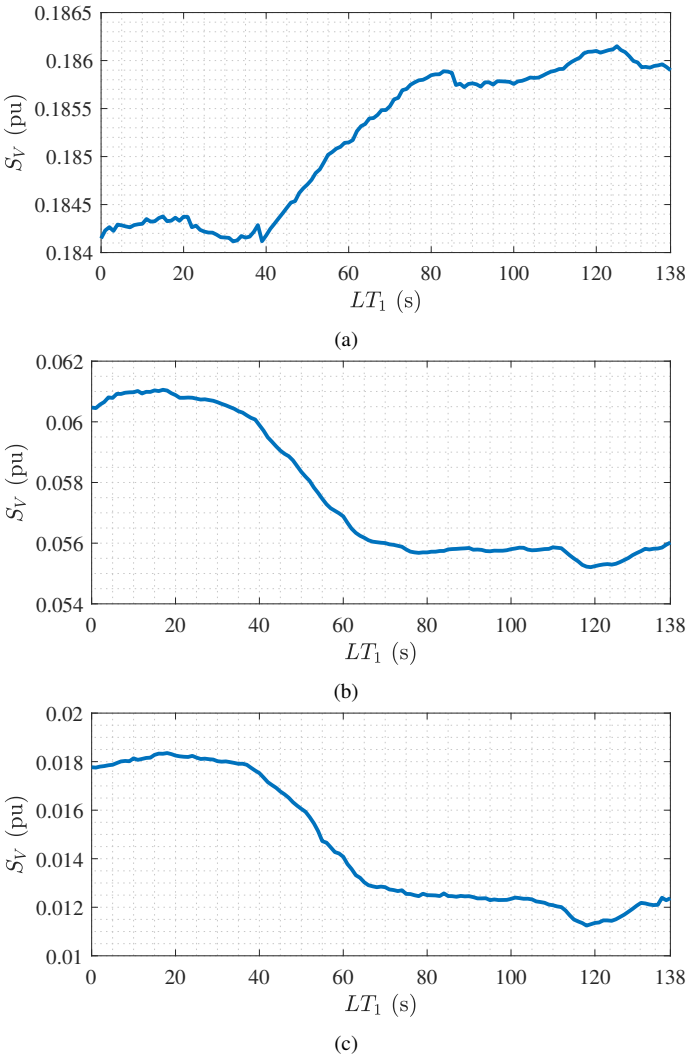


Fig. 9: $S_V$ index for all the value of of $LT_1$ Case A (a), Case B (b) and Case C (c).

## VII. Conclusion

This paper proposes a timetable adjustment approach to minimize the energy consumption of urban railway systems while ensuring effective regulation of the DC voltage of the traction network. Such an approach is formulated as a two-step procedure for the optimal allocation of layover time among train stops taking into account the operations of the adopted control strategy. Indeed, it is shown how the optimal adjustment of the timetable depends on the control nature. In the case of metro line 1 of Naples, the numerical results obtained for the proposed centralized control strategy have been compared with those concerning a conventional local strategy. They point out that regardless of the nature of the control, the optimal allocation of layover time can provide 7-8% reduction in energy consumption if compared with the worst allocation of layover time. In addition, the adoption of the proposed centralized control strategy, compared to the conventional local one, can provide a further 15% reduction in energy consumption.

## Appendix

### A. Power Flow Model in the case of Local Control and Limited Network Receptivity

DC railway systems typically adopt a local voltage regulation so that the catenary voltage does not exceed the prescribed limits, especially during train braking. Indeed, the injection of regenerative power causes the voltage rise in the traction network. Trains are, thus, forced to dissipate part of their regenerative power by rheostatic braking systems to bring the catenary voltage values within an acceptable range. Together with the presence of not-invertible substations, this significantly compromises the receptivity of the network.

Hence, assessing the behaviour of local control strategy in networks with limited receptivity requires solving a sequence of power flow equations, due to the recursive nature of the problem. Indeed, the first step is to assign the theoretical power of load buses and calculate train voltages according to the common power flow equations (6). For each time instant $k$, if no voltage exceeds the prescribed limits, the found solution is feasible thus further steps are not required. Otherwise, it needs adjusting trains power until getting a feasible solution of (6) for those $k$ that got an unfeasible solution. For instance, [26] proposed a power flow approach based on successive power reduction, which is effective but computationally intensive. [25] overcame this limitation by employing a sensitivity matrix approach to simultaneously adjust the regenerative power of all trains with over-voltages. In particular, herein the authors propose a different formulation for the approach provided by [25]. This approach was employed to study Case A in Section VI.

Once the power flow problem (6) has been solved by assigning the theoretical values of train regenerative power, it needs checking that all the resultant train voltages do not exceed prescribed limits. If the obtained solution does not match this condition, the regenerative power of trains with over-voltage must be reduced. Then, the power flow equations must be solved considering the new values of power and this procedure is repeated until all the voltage values are acceptable.

The power reduction is performed by means of the sensitivity matrix equation:

$$\mathbf{\Delta P}^{(m)} = \mathbf{H}^{(m)} \cdot \mathbf{\Delta V}^{(m)} \tag{31}$$

where $\mathbf{H}^{(m)}$ is the Jacobian of braking train power over-voltages w.r.t. their voltages, whereas the components of $\mathbf{\Delta V}^{(m)}$ and $\mathbf{\Delta P}^{(m)}$ are defined as follows

$$\begin{cases} \Delta V_{\mathrm{j}}^{(m)} = V_{\max} - V_{\mathrm{j}}^{(m)} \\ \Delta P_{\mathrm{j}}^{(m)} = P_{\mathrm{j}}^{(m+1)} - P_{\mathrm{j}}^{(m)} \end{cases} \tag{32}$$

It has to be noted that this is an iterative procedure, which is performed until $||\Delta V_{\mathrm{j}}^{(m)}|| \leq \varepsilon$, with $\varepsilon$ a suitable value of tolerance, whereas $m$ denotes the iteration counter.

Being $\mathcal{R}$ the subset of trains operating RB with over-voltages, let us define the vectors $\mathbf{V}_{\mathrm{L},\mathcal{R}}$ and $\mathbf{P}_{\mathrm{L},\mathcal{R}}$, whose

components are the elements $V_{\mathrm{L,j}}$ and $P_{\mathrm{L,j}}$ s.t. $\mathrm{j} \in \mathcal{R}$. This induces to sort vectors $\mathbf{V}_{\mathrm{L}}$ and $\mathbf{P}_{\mathrm{L}}$ s.t.:

$$\hat{\mathbf{V}}_{\mathrm{L}} = \begin{bmatrix} \mathbf{V}_{\mathrm{L},\mathcal{R}} \\ \mathbf{V}_{\mathrm{L},\mathcal{O}} \end{bmatrix} \quad \hat{\mathbf{P}}_{\mathrm{L}} = \begin{bmatrix} \mathbf{P}_{\mathrm{L},\mathcal{R}} \\ \mathbf{P}_{\mathrm{L},\mathcal{O}} \end{bmatrix} \tag{33}$$

where $\hat{(\cdot)}$ denotes the sorted vector and $\mathcal{O}$ is the subset of elements s.t. $\mathrm{j} \notin \mathcal{R}$. Mathematically, this operation can be expressed as follows

$$\begin{cases} \hat{\mathbf{V}}_{\mathrm{L}} = \mathbf{P}_{\pi}\mathbf{V}_{\mathrm{L}} \\ \hat{\mathbf{P}}_{\mathrm{L}} = \mathbf{P}_{\pi}\mathbf{P}_{\mathrm{L}} \end{cases} \tag{34}$$

where $\mathbf{P}_{\pi} \in \mathbb{R}^{n_{\mathrm{L}}}$ is the permutation matrix obtained by permuting the columns of the identity matrix. $\mathbf{P}_{\pi}$ is an orthogonal matrix, therefore the inverse coincides with the transpose matrix (i.e., $\mathbf{P}_{\pi}^{\mathrm{T}}$).

With reference to (6), the relation between trains' voltages and their powers can be expressed as follows

$$\mathbf{P}_{\mathrm{L}} = \mathrm{diag}\{\mathbf{V}_{\mathrm{L}}\}\mathbf{G}_{22}\mathbf{V}_{\mathrm{L}} + \mathrm{diag}\{\mathbf{V}_{\mathrm{L}}\}\mathbf{G}_{21}\mathbf{V}_{\mathrm{TPS}} \tag{35}$$

According to the sorting operation performed by (34), (35) can be rewritten as follows

$$\mathbf{P}_{\pi}\left(\mathrm{diag}\{\mathbf{V}_{\mathrm{L}}\}\mathbf{G}_{22}\right)\mathbf{P}_{\pi}^{\mathrm{T}}\hat{\mathbf{V}}_{\mathrm{L}} + \mathbf{P}_{\pi}\mathrm{diag}\{\mathbf{V}_{\mathrm{L}}\}\mathbf{G}_{21}\mathbf{V}_{\mathrm{TPS}} = \hat{\mathbf{P}}_{\mathrm{L}} \tag{36}$$

Thus, it can be shown that (36) can be rearranged as reported below[1]:

$$\mathrm{diag}\{\hat{\mathbf{V}}_{\mathrm{L}}\}\hat{\mathbf{G}}_{22}\hat{\mathbf{V}}_{\mathrm{L}} + \mathrm{diag}\{\hat{\mathbf{V}}_{\mathrm{L}}\}\hat{\mathbf{G}}_{21}\mathbf{V}_{\mathrm{TPS}} = \hat{\mathbf{P}}_{\mathrm{L}} \tag{37}$$

where

$$\hat{\mathbf{G}}_{22} = \mathbf{P}_{\pi}\mathbf{G}_{22}\mathbf{P}_{\pi}^{\mathrm{T}} \tag{38}$$

and

$$\hat{\mathbf{G}}_{21} = \mathbf{P}_{\pi}\mathbf{G}_{21} \tag{39}$$

A suitable partition for these matrices is represented by

$$\hat{\mathbf{G}}_{22} = \left[\begin{array}{c|c} \hat{\mathbf{G}}_{22,\mathcal{R}\times\mathcal{R}} & \hat{\mathbf{G}}_{22,\mathcal{R}\times\mathcal{O}} \\ \hline \hat{\mathbf{G}}_{22,\mathcal{O}\times\mathcal{R}} & \hat{\mathbf{G}}_{22,\mathcal{O}\times\mathcal{O}} \end{array}\right] \tag{40}$$

and

$$\hat{\mathbf{G}}_{21} = \left[\begin{array}{c} \hat{\mathbf{G}}_{21,\mathcal{R}} \\ \hline \hat{\mathbf{G}}_{21,\mathcal{O}} \end{array}\right] \tag{41}$$

Hence, the sensitivity matrix $\mathbf{H}^{(m)}$ is given by the following expression

$$\begin{aligned} \mathbf{H}^{(m)} = {} & \mathrm{diag}\{\hat{\mathbf{V}}_{\mathrm{L}}^{(m)}\}\hat{\mathbf{G}}_{22,\mathcal{R}\times\mathcal{R}} + \mathrm{diag}\{\hat{\mathbf{G}}_{22,\mathcal{R}\times\mathcal{R}}\hat{\mathbf{V}}_{\mathrm{L}}^{(m)}\} + \\ & + \mathrm{diag}\{\hat{\mathbf{G}}_{21,\mathcal{R}}\mathbf{V}_{\mathrm{TPS}}\} \end{aligned} \tag{42}$$

Thus, the over-voltages of all train is simultaneously adjusted according to (31) as long as the fixed tolerance is not respected.

[1]Let $\mathbf{D}$ and $\mathbf{P}_{\pi}$ be a diagonal matrix and a permutation matrix obtained by the permutation of the identity matrix columns, respectively. Then the following equality applies $\mathbf{P}_{\pi}\mathbf{D} = \mathbf{P}_{\pi}\mathbf{D}\mathbf{P}_{\pi}^{\mathrm{T}}\mathbf{P}_{\pi}$

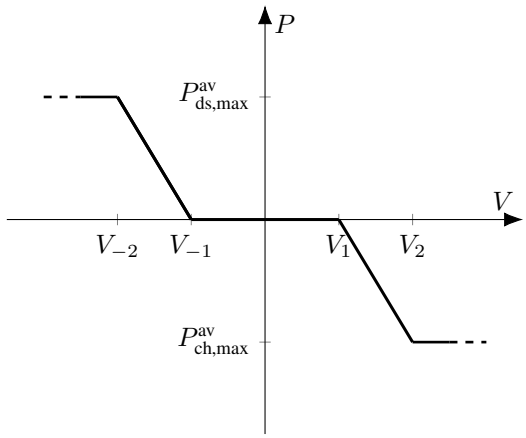


Fig. 10: Off-board storage *Voltage-Power* characteristic

### B. Local Control of Off-board Storage System

The off-board storage acts as a load/generator supporting the catenary voltage by injecting power when the local voltage falls below an assigned minimum value and absorbing power when the voltage exceeds the maximum value. Fig. 10 shows the *Voltage-Power* characteristic, where the charging power is assumed negative and the discharging positive. The abovementioned characteristic exhibits five distinct operative regions, defined by the voltage's values:

- $V_{-1} < V < V_1$: this is a region where the storage system does not operate, known as the dead band. It is designed to prevent unnecessary voltage adjustments within an acceptable range. As a result, it enables more effective control preventing the intermittent operation of the system;
- $V_{-2} < V \leq V_{-1}$: within this region, the storage system discharges. It has to be noted that the value of discharging power varies linearly with the voltage value;
- $V_1 \leq V < V_2$: within this region, the storage system charges. As in the previous operative region, here the power varies linearly with the voltage value;
- $V \leq V_{-2}$: if the voltage value drops down $V_{-2}$, the storage system supplies its maximum available discharging power (i.e., $P^{\mathrm{av}}_{\mathrm{ds,max}}$);
- $V \geq V_2$: if the voltage value exceeds $V_2$, the storage system absorbs its maximum available charging power (i.e., $P^{\mathrm{av}}_{\mathrm{ch,max}}$).

It has to be highlighted that the values of $P^{\mathrm{av}}_{\mathrm{ds,max}}$ and $P^{\mathrm{av}}_{\mathrm{ch,max}}$ depend on the value of SoC. Indeed, to avoid deep discharge and overcharge of the storage systems, typically some protections are adopted. They limit the charging/discharging power according to the value of SoC [27].

## REFERENCES

[1] M. Bozorg, A. Ahmadi-Khatir, and R. Cherkaoui, "Developing offer curves for an electric railway company in reserve markets based on robust energy and reserve scheduling," *IEEE Transactions on Power Systems*, vol. 31, no. 4, pp. 2609–2620, 2015.

[2] M. Bozorg, A. Ahmadi-Khatir, S. Cherkaoui, Rachid Kristijan, and A. Borna, "Effects of railway market liberalisation: European union perspective," *Sustainability*, vol. 14, no. 8, pp. 1–15, 2022.

[3] M. Cwil, W. Bartnik, and S. Jarzebowski, "Railway vehicle energy efficiency as a key factor in creating sustainable transportation systems," *Energies*, vol. 14, no. 4, pp. 1–13, 2021.

[4] H. Douglas, C. Roberts, S. Hillmansen, and F. Schmid, "An assessment of available measures to reduce traction energy use in railway networks," *Energy Conversion and Management*, vol. 106, pp. 1149–1165, 2015.

[5] N. Tian, S. Tang, A. Che, and P. Wu, "Measuring regional transport sustainability using super-efficiency sbm-dea with weighting preference," *Journal of Cleaner Production*, vol. 242, p. 118474, 2020.

[6] G. M. Scheepmaker, R. M. Goverde, and L. G. Kroon, "Review of energy-efficient train control and timetabling," *European Journal of Operational Research*, vol. 257, no. 2, pp. 355–376, 2017.

[7] A. González-Gil, R. Palacin, and P. Batty, "Sustainable urban rail systems: Strategies and technologies for optimal management of regenerative braking energy," *Energy Conversion and Management*, vol. 75, pp. 374–388, 2013.

[8] S. Gordon and D. Lehrer, "Coordinated train control and energy management control strategies," in *Proceedings of the 1998 ASME/IEEE Joint Railroad Conference*, 1998, pp. 165–176.

[9] M. Peña-Alcaraz, A. Fernández, A. P. Cucala, A. Ramos, and R. R. Pecharromán, "Optimal underground timetable design based on power flow for maximizing the use of regenerative-braking energy," *Proceedings of the Institution of Mechanical Engineers, Part F: Journal of Rail and Rapid Transit*, vol. 226, no. 4, pp. 397–408, 2012.

[10] Yang, Xin and Chen, Anthony and Li, Xiang and Ning, Bin and Tang, Tao, "An energy-efficient scheduling approach to improve the utilization of regenerative energy for metro systems," *Transportation Research Part C: Emerging Technologies*, vol. 57, pp. 13–29, 2015.

[11] Liu, Hongjie and Zhou, MengChu and Guo, Xiwang and Zhang, Zizhen and Ning, Bin and Tang, Tao, "Timetable Optimization for Regenerative Energy Utilization in Subway Systems," *IEEE Transactions on Intelligent Transportation Systems*, vol. 20, no. 9, pp. 3247–3257, 2019.

[12] Sun, Huijun and Wu, Jianjun and Ma, Hongnan and Yang, Xin and Gao, Ziyou, "A Bi-Objective Timetable Optimization Model for Urban Rail Transit Based on the Time-Dependent Passenger Volume," *IEEE Transactions on Intelligent Transportation Systems*, vol. 20, no. 2, 2019.

[13] Wang, Pengling and Bešinović, Nikola and Goverde, Rob MP and Corman, Francesco, "Improving the Utilization of Regenerative Energy and Shaving Power Peaks by Railway Timetable Adjustment," *IEEE Transactions on Intelligent Transportation Systems*, 2022.

[14] Liu, Wei and Zhang, Jian and Wang, Hui and Wu, Tuojian and Lou, Ying and Ye, Xiaowen, "Modified AC/DC Unified Power Flow and Energy-Saving Evaluation for Urban Rail Power Supply System With Energy Feedback Systems," *IEEE Transactions on Vehicular Technology*, vol. 70, no. 10, pp. 9898–9909, 2021.

[15] M. Botte, L. D'Acierno, A. Di Pasquale, F. Mottola, and M. Pagano, "Optimal motion of a rolling stock fleet under traction power system constraints," *IEEE Transactions on Transportation Electrification*, 2022.

[16] T. Kulworawanichpong, "Multi-train modeling and simulation integrated with traction power supply solver using simplified newton–raphson method," *Journal of Modern Transportation*, vol. 23, no. 4, pp. 241–251, 2015.

[17] M. Khodaparastan, O. Dutta, M. Saleh, and A. A. Mohamed, "Modeling and simulation of dc electric rail transit systems with wayside energy storage," *IEEE Transactions on Vehicular Technology*, vol. 68, no. 3, pp. 2218–2228, 2019.

[18] L. D'Acierno and M. Botte, "Railway system design by adopting the Merry-Go-Round (MGR) paradigm," *Sustainability*, vol. 13, no. 4, pp. 1–21, 2021.

[19] Arboleya, Pablo and Mohamed, Bassam and González-Morán, Cristina and El-Sayed, Islam, "BFS algorithm for voltage-constrained meshed DC traction networks with nonsmooth voltage-dependent loads and generators," *IEEE Transactions on Power Systems*, vol. 31, no. 2, pp. 1526–1536, 2015.

[20] V. A. Kleftakis and N. D. Hatziargyriou, "Optimal control of reversible substations and wayside storage devices for voltage stabilization and energy savings in metro railway networks," *IEEE Transactions on Transportation Electrification*, vol. 5, no. 2, pp. 515–523, 2019.

[21] Roch-Dupré, David and López-López, Álvaro J and Pecharromán, Ramón R and Cucala, Asunción P and Fernández-Cardador, Antonio, "Analysis of the demand charge in DC railway systems and reduction of its economic impact with Energy Storage Systems," *International Journal of Electrical Power & Energy Systems*, vol. 93, pp. 459–467, 2017.

[22] A. Andreotti, A. Di Pasquale, M. Pagano, N. Ravichandran, and F. Volpe, "An optimal centralized control strategy for regenerative braking energy flow exchanges in dc railway traction systems," in *2022 International Symposium on Power Electronics, Electrical Drives, Automation and Motion (SPEEDAM)*. IEEE, 2022, pp. 436–441.

[23] E. CENELEC, "50163," *Railway applications–Supply voltages of traction systems*, 2013.

[24] Gulin, Marko and Vašak, Mario and Baotić, Mato, "Analysis of microgrid power flow optimization with consideration of residual storages state," in *2015 European Control Conference (ECC)*. IEEE, 2015, pp. 3126–3131.

[25] Jabr, Rabih A and Džafić, Izudin, "Solution of DC railway traction power flow systems including limited network receptivity," *IEEE Transactions on Power Systems*, vol. 33, no. 1, pp. 962–969, 2017.

[26] j. Cai, Yueming and Irving, MR and Case, SH, "Iterative techniques for the solution of complex DC-rail-traction systems including regenerative braking," vol. 142, no. 5, pp. 445–452, 1995.

[27] P. Arboleya, B. Mohamed, and I. El-Sayed, "Dc railway simulation including controllable power electronic and energy storage devices," *IEEE Transactions on Power Systems*, vol. 33, no. 5, pp. 5319–5329, 2018.


**Marilisa Botte** was born in Caserta, Italy, in 1988. She received the M.Sc. degree in hydraulics and transportation systems engineering, in 2014 and the Ph.D. degree in civil system engineering, in 2018, both from Federico II University of Naples, Italy. Currently, she is Assistant Professor at Federico II University of Naples, Italy. She has authored more than 50 papers in peer-reviewed journals and conference proceedings. Her research interests include sustainable mobility, MaaS systems, transportation and urban planning, rail system analysis and management, energy-saving strategies. interests.

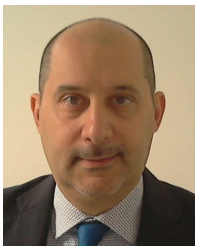

**Luca D'Acierno** was born in Naples, Italy, in 1974. He holds an MSc degree in civil engineering (2000) and a PhD in road infrastructures and transportation systems (2003), both from Federico II University of Naples, Italy. Currently, he is Associate Professor at Federico II University of Naples, Italy. He has authored more than 170 papers in peer-reviewed journals and conference proceedings. His research interests include public transport planning and design, rail system analysis and management, multimodal transportation network design, transportation network assignment, pricing policy analysis, energy saving strategies, and probe vehicle use.

**Antonio Di Pasquale** was born in Naples, Italy, in 1995. He received the M.S. degree with honors in electrical engineering from the University of Cassino and and Southern Lazio, in 2019. Since 2020, he has been Ph.D. Student with the Electrical Engineering and Information Technology Department at the University of Naples Federico II. His research interests primarily focus on electrical systems for mobility and optimization strategies for controlling railway systems.

**Fabio Mottola** (M' 07, SM' 18) received the M.Sc. with honors and Ph.D. degrees in Electrical Engineering from the University of Naples Federico II, Naples, Italy, in 2004 and 2008, respectively. Currently, he is Assistant Professor at the Department of Electrical Engineering and Information Technology of the University of Naples Federico II. His research interests mainly focus on the integration of renewable energy sources and energy storage devices in power systems.

**Mario Pagano** (SM' 17) was born in Naples, Italy, in 1970. He received the M.Sc. (Hons.) and the Ph.D. degree in electrical engineering from the University of Naples Federico II, Italy, in 1995 and 1999, respectively. In 2002, he was appointed researcher with power systems at the University of Naples Federico II, Italy. He is currently Associate Professor. He is author or co-author of over 120 scientific papers published in reviewed journals and presented at international and national conferences; his research interests include transmission power systems, renewable sources, storage systems and electrical systems for mobility.